

Abbasi, Q. H., El Sallabi, H., Chopra, N., Yang, K., Qaraqe, K. A. and Alomainy, A. (2016) Terahertz channel characterization inside the human skin for nano-scale body-centric networks. *IEEE Transactions on Terahertz Science and Technology*, 6(3), pp. 427-434.  
(doi:[10.1109/TTHZ.2016.2542213](https://doi.org/10.1109/TTHZ.2016.2542213))

This is the author's final accepted version.

There may be differences between this version and the published version. You are advised to consult the publisher's version if you wish to cite from it.

<http://eprints.gla.ac.uk/141057/>

Deposited on: 03 July 2017

# Terahertz Channel Characterisation Inside the Human Skin for Nano-scale Body-Centric Networks

Qammer H. Abbasi, *Senior Member, IEEE*, Hassan El Sallabi, *Member, IEEE*, Nishtha Chopra, *Student Member, IEEE*, Ke Yang, *Student Member, IEEE*, Khalid Qaraqe, *Senior Member, IEEE*, Akram Alomainy, *Senior Member, IEEE*

**Abstract**—This paper focuses on the development of novel radio channel model inside the human skin at the terahertz range, which will enable the interaction among potential nano-machines operating in the inter cellular areas of the human skin. Thorough studies are performed on the attenuation of electromagnetic waves inside the human skin, while taking into account the frequency of operation, distance between the nano-machines and number of sweat ducts. A novel channel model is presented for communication of nano-machines inside the human skin and its validation is performed by varying the aforementioned parameters with a reasonable accuracy. The statistics of error prediction between simulated and modeled data are: mean ( $\mu$ ) = 0.6 dB and standard deviation ( $\sigma$ ) = 0.4 dB, which indicates the high accuracy of prediction model as compared with measurement data from simulation. In addition, the results of proposed channel model are compared with Terahertz Time Domain Spectroscopy based measurement of skin sample and the statistics of error prediction in this case are:  $\mu = 2.10$  dB and  $\sigma = 6.23$  dB, which also validates the accuracy of proposed model. Results in this paper highlight the issues and related challenges while characterizing the communication in such a medium, thus paving the way towards novel research activities devoted to the design and the optimization of advanced applications in the health-care domain.

**Keywords**—Nanoscale communications, Body Area Nano Network, channel characterisation, Internet of Nano-things

## I. INTRODUCTION

With the growing demand of nanotechnology in all the domains of science and engineering, its gaining enormous attention from the various disciplines and domains. The connectivity of the nano-devices to conduct complex tasks lead to the proposal of the nano-networks, followed by the concept of nano-communication [1]. Main applications of nano-networks are categorised as, but are not limited to biomedical,

environmental, industrial and military [2], which can also be extended into other fields like consumer electronics, life style and home appliances. Its application in medical diagnostics and treatment has a quite bright future, because of its ability to access small and delicate body sites non invasively, where conventional medical devices fall short [3]. Electromagnetic based communications, handled in the terahertz band, are considered a viable technique for supporting data exchange in the nano-machines [4]. While almost all other portions of spectrum are already deployed in the medical applications, the properties of Terahertz (THz) band open a new era and interest, because of its non ionization hazards for biological tissues and less susceptibility to some of propagation effects (*i.e.*, Rayleigh scattering etc) [5].

Body-centric wireless communication (BCWC) has been extensively studied in the past for a range of frequencies [6], [7], however the need to reduce the size of the devices makes nano-scale technologies attractive for future applications. This opens up opportunities of applying nano-devices made of the novel materials, like carbon nano tubes (CNT), graphene, [8] which operate at THz frequencies and probably inside human bodies. Since, terahertz radiation can detect the fine variations in the water contents and other biomaterial tissues as the molecular resonances are existing and can be detected in this frequency range. Consequently, one of the emerging areas of research is analysing the propagation of terahertz electromagnetic waves through the skin tissues to develop a diagnostic tools for early detection and treatment of abnormalities with the skin tissues as a sign of skin cancer [9]. Several studies on the applicability of THz communication for biomedical applications are performed in [10]–[13]. The optical parameters of human tissues up to 2.5 THz have been empirically characterized in [10], while the possibility of applying EM waves in nano-networks is presented in [13]. Jornet *et al.* [12] studied the THz channel model in the air by varying water vapor concentration and also proposed a new physical-layer aware medium access control (MAC) protocol [14]. The characteristics of electromagnetic waves propagating inside human body at terahertz frequencies have been studied in [15], which shows that path loss has a relation with the dielectric loss of human tissues. In [16], the electrical properties (conductivity and permittivity values) of each layer have been investigated depending on the water content of each layer.

Though there are some initial studies presented in literature about THz channel modeling, but to the best of authors' knowledge, there are no explicit investigation performed about

---

This publication was made possible by NPRP grant # 7-125-2-061 from the Qatar National Research Fund (a member of Qatar Foundation). The statements made herein are solely the responsibility of the authors. The HPC resources used in this work were provided by the IT Research Computing group in Texas A & M University at Qatar, which is funded by Qatar Foundation for Education, Science and Community Development.

Qammer, Khalid and Hassan are with the Dep. of Electrical and Computer Engineering, Texas A & M University at Qatar. Qammer is also with Queen Mary University of London and UET, Lahore.; e-mail: {qammer.abbasi; hassan.el\_sallabi, k.qaraqe}@tamu.edu.

Nishtha Chopra, Ke Yang and A. Alomainy are with Antennas & Electromagnetics School of Electronic Engineering and Computer Science Queen Mary University of London, London; e-mail: {n.chopra, ke.yang; a.alomainy}@qmul.ac.uk.

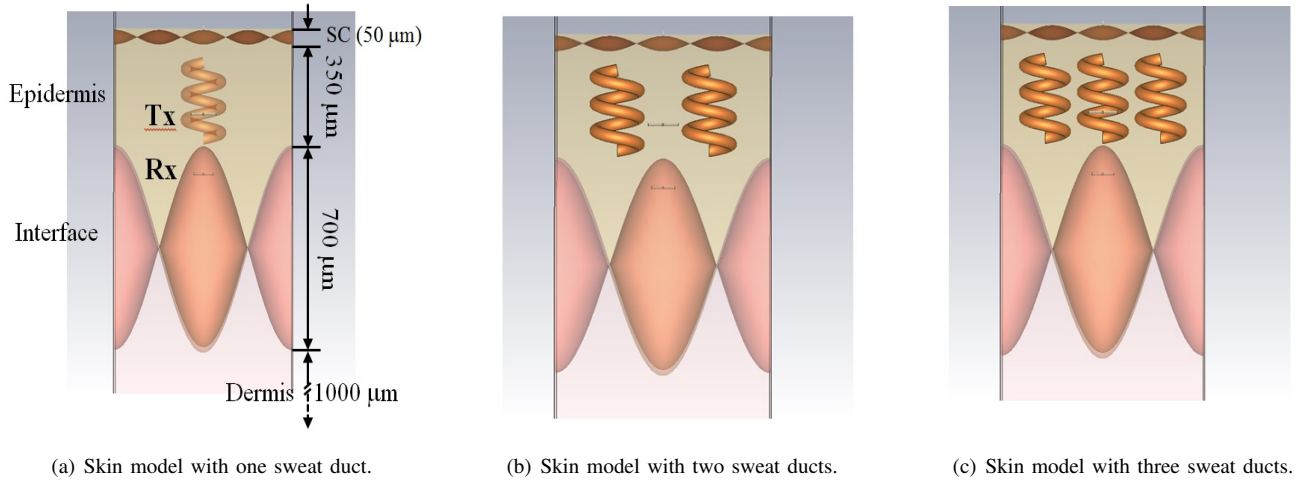


Fig. 1. Numerical skin model (based on CST Microwave Studio<sup>TM</sup>) representing the layers and their thickness, while including different number of sweat ducts (dimensions for each layer are shown as well [17]).

the EM channel modeling inside the skin at THz, while taking into account the number of sweat ducts, frequency and distance dependant characteristics. In this paper, a novel channel model is proposed for inside the skin, which takes into account all of the aforementioned parameters and the blind testing is performed on the proposed model for validating the analytical results with the simulated data. In addition, the proposed model is also validated by comparing it with the measurement results of skin sample using Terahertz Time Domain Spectroscopy (THz TDS).

The rest of paper is organized as follows. Section II highlights the details of skin model used in this study. Section III details about the proposed channel model, in addition to its validation by blind testing and THz TDS data and Finally, conclusions are drawn in section IV.

## II. SIMULATION AND MEASUREMENT SETTINGS

### A. Numerical Human Skin Model

The skin is a complex heterogeneous and anisotropic medium, where the small parts, like blood vessel and pigment content, are spatially distributed in depth [18]. In this study, the skin tissues were represented by three layer model (*i.e.*, stratum corneum (SC), epidermis, and dermis). The dimensions are shown in Fig. 1) and the roughness of boundaries between the SC and epidermis was considered in the skin model as the order of magnitude for THz wavelength and roughness dimensions were comparable [17]. Since, sweat glands are distributed almost all over the human body and represent a form of cooling in humans. Hence their consideration in the model was essential to get a closer insight of EM wave propagation inside the real human tissue and their effect on the signal propagation losses through the skin. The Optical coherent tomography imaging [19] of human skin shows that the sweat ducts are of spiral shape. The detailed model of human skin with sweat duct is initially presented by Hayut *et*

*al.* in [19]. In this study, the sweat duct was modeled in the epidermis layer [19] by a helix [17] as shown in Fig. 1 with a height of  $265 \mu m$  and diameter equals to  $40 \mu m$ . As, only when the sweat duct contains sweat, containing 99% water and 1% salt and amino acid [20], it can be regarded as a conductor; and hence the permittivity of water at THz band was used to model sweat duct. In real skin tissues, the thickness of each layer is differed according to the position all over the body, ranging from very thin, when covering sensitive areas of the body, such as eyelids, to very thick when covering the tough areas, such as the hand palm. The skin tissue dimensions in the model were taken to be average between the skin dimensions of the sensitive areas and the tough areas. Two dipoles optimised to ensure that the impedance matching is better than  $-10 dB$  (modeled as nano antennas working at THz band) were used as transmit (Tx) and receive (Rx) antennas, where one was placed in the epidermis and other was located in the dermis layer. Two discrete ports were applied to the dipoles and the transmission coefficient,  $S_{21}$ , was recorded from 0.8 - 1.2 THz. Fig. 1 represents the skin layer model studied in this paper with different spacing between the Tx and Rx by varying number of sweat ducts. The simulations are performed in CST Microwave Studio<sup>TM</sup> and due to large simulation domain and large number of mesh cells for the human skin, simulations were run on a high performance computing cluster named "RAAD". RAAD is a 42+ TFLOP system with blade-based Linux HPC cluster containing upwards of 2,200 traditional Intel CPU cores with 12 NVIDIA TESLA K20 GPUs, each with 2,496 CUDA cores. RAAD is running portable batch system (PBS) for job scheduling. In addition, FAT nodes offer 32 CPU cores coupled with 256 GB of RAM on a single motherboard, catering to a certain class of parallel workloads, or workloads with unusually large memory requirements. The majority of the cluster's compute nodes are comprised of 16-core servers with 64 GB of RAM and a single 128 GB SSD on each server. In this study simulations were performed using 32

CPUs with 32 GB of memory for each individual simulation and more than 50 such simulations were run on the RAAD cluster.

### B. Terahertz Time Domain Spectroscopy of The Human Skin

The Terahertz Time Domain Spectroscopy (THz-TDS) at Queen Mary University of London (QMUL) [21] has a typical range of 0.1- 4 THz, which provides access to broader spectral analysis (schematic of this system is shown in Fig. 2). The THz-TDS system is a carefully designed assembly of the following components - Ti:Sapphire is the femtosecond pulsed laser with adjustable wavelength range of 750 - 850 nm; pulse repetition rate of 80 MHz and peak power is about 1 W. The delay stage has maximum travel distance of 15 cm. THz emitter is LT-GaAs photoconductive antenna with a biased voltage of 200 V and a gap size of approximately 0.5 mm, which makes the laser beam positioning relatively easier. A ZnTe crystal is employed as an electro-optic detector with thickness of 2 mm, which allows enough interaction length of probe beam and THz wave in the crystal. The sample consist of two layers: epidermis and dermis, however, epidermis is very thin in comparison to dermis. The samples are wedged between two TPX (Polymethylpentene) slabs with a spacer of known thickness. TPX is used as a sample holder, since it is transparent to THz radiation; the light is mostly transmitted through the sample with minimal absorption in TPX [22]. These measurements are performed applying the aforementioned THz TDS system and therefore phase and amplitude information are collected and later on post processed using transfer equation based algorithm for calculating pathloss and other material parameters [23]. The TDS pulses are generated and detected via mode locked laser. The lock-in amplifier locks and records the detected THz data aided by a computer-generated program written in LabView<sup>TM</sup>. In this study, the incoming THz signal consists of total 1024 consecutive samples, which are recorded at each position of the delay stage. THz-time domain data takes the form of a single pulse, with a period of 1 picosecond, followed by a series of attenuated pulses arising either from reflections at the interface of components within the TDS system, or from etalon reflections within the sample itself. Measurements are repeated several times with same sample to ensure repeatability.

Analogous to the human skin tissue, artificial synthesis of collagen was done in a controlled environment at Subcutaneous Group Blizzard Institute, Queen Mary University of London. Collagen forms the second layer of human skin (*i.e.*, dermis) and is thickest most layer of the skin. It provides scaffolding for essential cells and structures including blood vessels, lymph vessels, hair follicles and sweat glands. Collagen type 1 is extracted from the rat-tail is a heterotrimer consisting of two ( $\alpha$ -1) chains and one ( $\alpha$ -2) chains [24]. Collagens can be readily isolated from animal tissues, stored in solution or as a solid, and used as biocompatible coatings or soft-tissue substitutes that can protect and support damaged tissues. The synthesis of collagen (as shown in Fig. 3) was done with a help of standard recipe with total stock solution of 3.35 mg/ml out of which 80% is collagen. The solution was thoroughly

mixed and separated into sections of 6-well plate. The gels are incubated (5% CO<sub>2</sub>) at 37° C to support the growth of the cells. Fig. 3 also shows the microscopic view of growth of collagen layer. As mentioned above the artificially cultured collagen samples were wedged between TPX window with a spacer of 0.2 mm, thus keeping the thickness of the sample constant for THz TDS measurement.

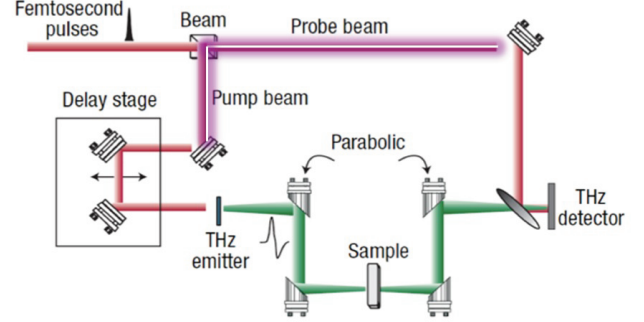


Fig. 2. Schematic of Terahertz Time Domain Spectroscopy setup at Queen Mary University of London, which is used for skin sample measurement [24].

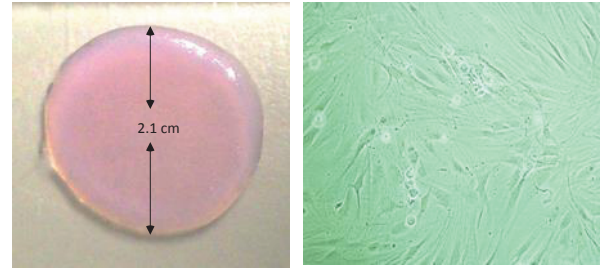


Fig. 3. Artificially synthesized collagen layer at the Blizzard Institute, QMUL which was used for measurement (left) & Fibroblast cells assisting the growth of collagen layer (right) [24].

### III. TERAHERTZ CHANNEL MODELING INSIDE THE SKIN

A modified Friis equation has been proposed by Jornet et al. in [12] to calculate the path loss of the THz channel in water vapor, which can be divided into two parts: the spreading path loss  $PL_{spr}$ , which is due to the expansion of waves inside the tissue and the absorption path loss  $PL_{abs}$  (due to absorption of waves in tissue). Similarly, the path loss in human tissues can also be divided into two parts:

$$PL_{total}[dB] = PL_{spr}(f, d)[dB] + PL_{abs}(f, d)[dB] \quad (1)$$

$$= 20 \log \frac{4\pi d}{\lambda_g} + 10\alpha d \log e \quad (2)$$

where,  $f$  stands for the frequency,  $d$  is the path length,  $\alpha = 4\pi K/\lambda$ , where  $K$  is extinction coefficient, which measures the amount of absorption loss. In this study, the electromagnetic power is considered to spread spherically with distance. This path loss model takes into account only distance and frequency

and it doesn't explicitly discuss about inside the skin. This paper presents a novel model inside the human skin by considering additional parameters, which also plays a vital role in varying channel characteristics.

#### A. Proposed Channel Model

In order to infer the path loss model from measurement data, investigation on the correlation level between measurement data and explanatory variables of propagation environment is needed, *i.e.*, distance, number of ducts and frequency. The relationship between distance and measured path loss varies with distance model and different models are investigated to find out the model that has highest correlation level. This indicates highest level of information captured by model from measured path loss. As a first step, the correlation with distance in logarithmic scale is tested. The correlation level between path loss ( $PL$ ) in dB scale and distance in logarithmic domain is 0.98. In order to find out, if the  $PL$  follows other distance models, the correlation of measured  $PL$  with  $d^\alpha$  is investigated. Figure 4(a) shows variation of correlation level with exponent of distance model  $\alpha$ . Result shows that there are some values of  $\alpha$ , where the distance model  $d^\alpha$  has higher correlation level than the logarithmic distance model, *i.e.*,  $\log_{10}(d)$ . In order to find the value of  $\alpha$  that has highest correlation level, a model of correlation level ( $C$ ) has been inferred from correlation level data as a function of  $\alpha$ . The model is given as:

$$C(\alpha) = 0.00181\alpha^3 - 0.018\alpha^2 + 0.021\alpha + 0.984 \quad (3)$$

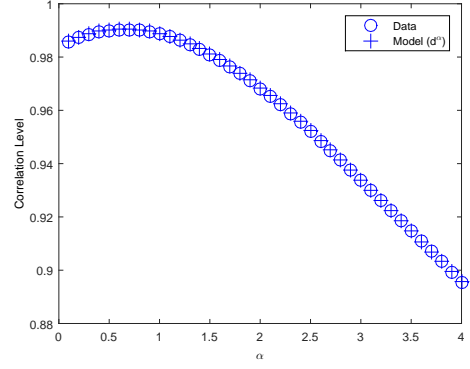
The distance model that has highest correlation is the model that has  $\alpha$ , which fulfills  $\frac{dC}{d\alpha} = 0$ . The solution of this equation is  $\alpha = 0.65$ , which leads to correlation value of 0.9903. The correlation level fitting of eq. 3 is shown in Figure. 4(a).

An interim distance model ( $d^{0.65}$ ) is used to extract the information of PL data that are not function of distance model as the error between the PL and the interim distance model. Then, this extracted residual is tested against frequency as an explanatory model variable to check, if it has any correlation. This correlation between the residual of PL after excluding the effect of distance model and frequency model is tested against frequency models of  $\log_{10}(f)$  and  $f^\gamma$ . The correlation level with  $\log_{10}(f)$  is 0.94 and with frequency models different values of  $\gamma$  is shown in Fig. 4(b). It is clear from the figure that there are some values of  $\gamma$ , where frequency model has higher correlation than the model  $\log_{10}(f)$ . In order to find the value that has the highest correlation value, the correlation level is modeled as function of  $\gamma$  and is given as:

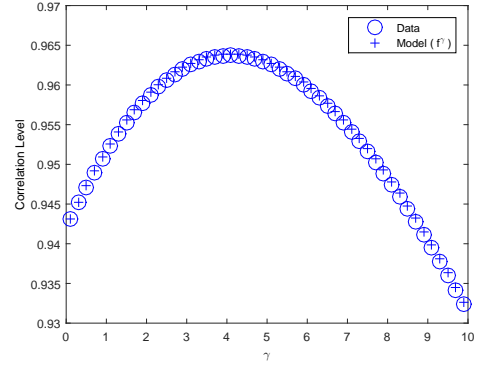
$$C_f(\gamma) = 3.97 * 10^{-5}\gamma^3 - 0.00164\gamma^2 + 0.0114\gamma + 0.942 \quad (4)$$

The value of  $\gamma$ , which gives highest correlation for frequency model is obtained from  $\frac{dC_f}{d\gamma} = 0$ , which is  $\gamma = 4.07$ .

In order to find  $PL$  model as function of multi variables, a multivariable regression technique has been invoked. This is to find the relationship between two or more explanatory variables by fitting a linear equation to the collected data. After



(a) Correlation level fitting of  $\alpha$



(b) Correlation level fitting of  $\gamma$

Fig. 4. Correlation level fitting of eq. 3 and eq. 4, which is used to calculate the value of  $\alpha$  (distance model) and  $\gamma$  (frequency model), which is the maximum value in fitting.

intensive experiments, it turns out that the model should be of the form:

$$PL = A(N) + B(N)d^{0.65} + C(N)f^{4.07} \quad (5)$$

Where the regression technique is used to find the functions of  $A(N)$ ,  $B(N)$ , and  $C(N)$ , which are the constant offset, coefficients of distance and frequency as functions of number of ducts, respectively. The modeling process is conducted in two steps: (i) the fitting process is done for fixed values of  $N$ , and model fitting is performed for corresponding data of  $PL$ . (ii) a series of data for  $A$ ,  $B$  and  $C$  corresponding to various values of  $N$ , is modeled as affine functions of  $N$ . The fitting process is based on least squares fit for particular value of  $N$ , which can be formulated as:

$$PL = X\beta \quad (6)$$

$$X = \begin{bmatrix} 1 & d_1^{0.65} & f_1^{4.07} \\ 1 & d_2^{0.65} & f_2^{4.07} \\ \vdots & \vdots & \vdots \\ 1 & d_n^{0.65} & f_n^{4.07} \end{bmatrix} \quad (7)$$

TABLE I. FITTING STATISTICS OF THE PROPOSED MODEL WITH RESPECT TO MEASUREMENT

Correlation Level	R-squared	Adjusted R-squared	RMSE
0.9993	0.9987	0.9987	0.3407

$$\beta = \begin{bmatrix} A1 \\ B1 \\ C1 \end{bmatrix} \quad (8)$$

$$PL = \begin{bmatrix} PL_1 \\ PL_2 \\ \vdots \\ PL_n \end{bmatrix} \quad (9)$$

The goal here is to find the best values of  $A_i$ ,  $B_i$  and  $C_i$  for each value of  $N = i$ , that minimizes the difference between left and right sides such that:

$$\hat{\beta} = \min_{\beta} S(\beta), \quad (10)$$

$$S(\beta) = \|PL - X\beta\| \quad (11)$$

$S$  is the objective function that has to be solved using quadratic minimization problem since eq. 5 has no solution. The solution of this optimization problem (eq. 11) is well-known and is given as [25]:

$$\hat{\beta} = (X^T X)^{-1} X^T PL \quad (12)$$

Then, each coefficients ( $A_i$ ,  $B_i$  and  $C_i$ ) for different values of  $N$  is fitted with affine function of  $N$  as follows:

$$A(N) = a_1 + b_1 N, \quad (13)$$

$$B(N) = a_2 + b_2 N, \quad (14)$$

$$C(N) = a_3 + b_3 N \quad (15)$$

The final form of the path loss model inferred from measurement data after the two described fitting process is given as:

$$PL = -0.2 * N + 3.98 + (0.44 * N + 98.48)d^{0.65} + (0.068 * N + 2.4)f^{4.07} \quad (16)$$

Where,  $f$  is frequency in THz,  $d$  is distance in mm, and  $N$  is number of sweat ducts, respectively.

The fitting statistics of the proposed model is shown in Table I using R-squared, coefficient of determination, which is a measure of how close a statistical model to the measurement data. However, the R-squared does not determine whether the estimates of the prediction coefficients are biased. It also may mislead the goodness of fit as a result of overfitting process. These problems are addressed in Adjusted R-squared measure which adjusts the number of explanatory variables to the measurement data. This is important measure in multi-variable linear regression since it penalizes the model for adding more nonsense variables. The root mean squared error (RMSE) is an absolute measure of close the model to the measurement data. It can be interpreted as the standard deviation of unexplained and un-modeled variation in data. The lower value of RMSE is the better fit.

## B. Performance Evaluation of Proposed Model

In order to test the performance of the model against blind data (where number of ducts, distance and frequency was unknown) that has not been used in fitting data, a new experiment was conducted to test further of level of blind measurement data that has both new value of number of duct at different measurements distances. Figure 5(a) shows the comparison of modeled path loss with the measured data for different values of number of ducts for different distances and frequency ranges. Figs. 5(b) and 5(c) shows the comparison of modeled and measured data for different variables of the model distance and frequency, respectively. Figure 5(d) shows the prediction error between blind path loss data (*i.e.*, data which was not used in fitting and derivation process of path loss model) and that predicted by the path loss model and are given as: mean error is 0.6 dB, and its standard deviation is 0.4 dB. This all indicates the high accuracy of prediction model as compared with the measured data from the simulation, which have not been used in formulating the proposed model.

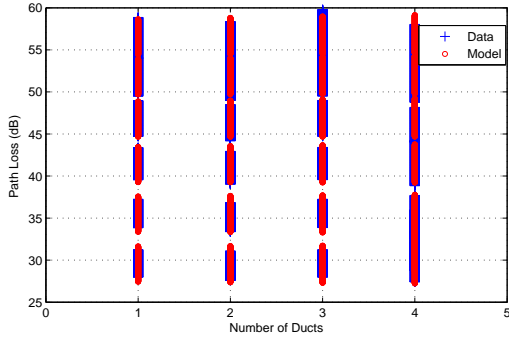
## C. Comparison of Proposed Model with Measurement Studies

The human skin sample absorption is measured using the THz TDS system (the details about measurement are given in Section II-B). The material properties *i.e.*, refractive index and absorption coefficient are calculated using details given in [24]. The total path loss is calculated by converting the measured time domain data to frequency domain by applying fast fourier transform and then averaging it across the band of interest [12], [15] for THz channel inside the skin. The measured sample pathloss results are compared with the modeled pathloss as per eq. 16 (Section III-A). Fig. 6 shows comparison of measured and modeled path loss for inside the skin. The statistics of prediction error between the THz TDS based skin sample measurement and modeled pathloss are given as: mean error is 2.10 dB, and its standard deviation is 6.23 dB. This indicates the high accuracy of prediction model as compared to measurement data.

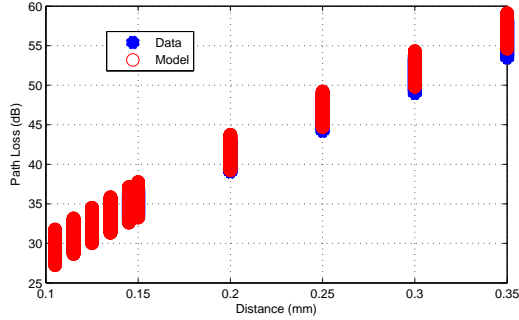
## IV. CONCLUSIONS

In this paper a novel path loss model is proposed inside the human skin at terahertz frequencies by considering different distances, number of sweat ducts and frequencies. A blind testing is performed on the proposed model and comparison is performed with the data from simulation with a very good agreement. Also the comparison of proposed model with the THz TDS measurement results show a reasonable agreement with the statistics of error prediction in this case are:  $\mu = 2.10 \text{ dB}$  and  $\sigma = 6.23 \text{ dB}$ . This all validates the accuracy of proposed channel model inside the human skin. The reported analysis highlights the novel method to cater the communication challenges in such environment and paved a way for further studies in this harsh environment, even combined with hybrid molecular communication techniques for health-care applications.

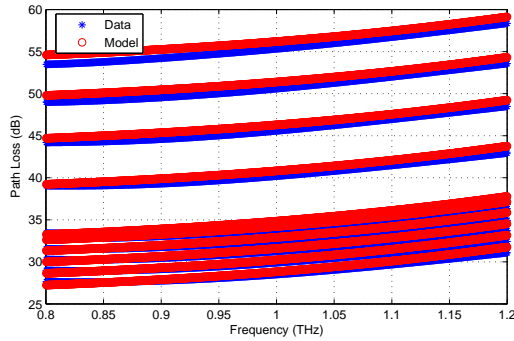




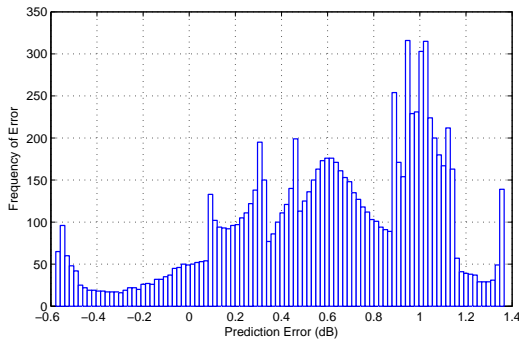
(a) Path loss with respect to number of ducts ( $N$ )



(b) Path loss with respect to distance at  $N = 4$



(c) Path loss with respect to frequency for different distances at  $N = 4$



(d) Prediction Error of proposed model with actual input data

Fig. 5. Blind testing of proposed model by varying number of ducts, distance and frequency, while comparing to measured data and the prediction error.

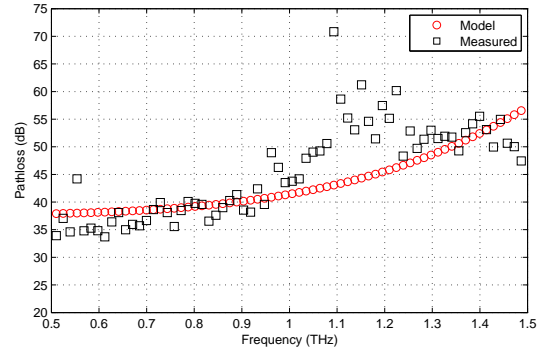


Fig. 6. Comparison of measured (THz TDS) and modeled path loss inside the skin at THz frequencies.

## REFERENCES

- [1] S. F. Bush, *Nanoscale Communication Networks*. Artech House, 2010.
- [2] I. F. Akyildiz, F. Brunetti, and C. Blázquez, "Nanonetworks: A new communication paradigm," *Computer Networks*, vol. 52, no. 12, pp. 2260–2279, 2008.
- [3] M. Sitti, H. Ceylan, W. Hu, J. Giltinan, M. Turan, S. Yim, and E. Diller, "Biomedical applications of untethered mobile milli/microrobots," *Proceedings of the IEEE*, vol. 103, no. 2, pp. 205–224, 2015.
- [4] S. Balasubramaniam and J. Kangasharju, "Realizing the internet of nano things: Challenges, solutions, and applications," *Computer*, vol. 46, no. 2, pp. 62–68, Feb 2013.
- [5] G. Piro, K. Yang, G. Boggia, N. Chopra, L. Grieco, and A. Alo-mainy, "Terahertz communications in human tissues at the nano-scale for healthcare applications," *IEEE Transactions on Nanotechnology*, vol. 14, no. 3, pp. 404–406, 2015.
- [6] P. S. Hall and Y. Hao, *Antennas and Propagation for Body-Centric Wireless Communication*. Artech House, 2012.
- [7] Q. H. Abbasi, A. Sani, A. Alomainy, and Y. Hao, "Numerical characterization and modeling of subject-specific ultrawideband body-centric radio channels and systems for healthcare applications," *Information Technology in Biomedicine, IEEE Transactions on*, vol. 16, no. 2, pp. 221–227, 2012.
- [8] S. Luryi, J. Xu, and A. Zaslavsky, *Future Trends in Microelectronics: Frontiers and Innovations*. John Wiley & Sons, 2013.
- [9] T. Binzoni, A. Vogel, A. H. Gandjbakhche, and R. Marchesini, "Detection limits of multi-spectral optical imaging under the skin surface," *Physics in medicine and biology*, vol. 53, pp. 617–636, 2008.
- [10] E. Berry, A. J. Fitzgerald, N. N. Zinov'ev, G. C. Walker, S. Homer-Vanniasinkam, C. D. Sudworth, R. E. Miles, J. M. Chamberlain, and M. A. Smith, "Optical properties of tissue measured using terahertz-pulsed imaging," in *Medical Imaging 2003*. International Society for Optics and Photonics, 2003, pp. 459–470.
- [11] A. Fitzgerald, E. Berry, N. Zinov'ev, S. Homer-Vanniasinkam, R. Miles, J. Chamberlain, and M. Smith, "Catalogue of human tissue optical properties at terahertz frequencies," *Journal of Biological Physics*, vol. 29, no. 2-3, pp. 123–128, 2003.
- [12] J. M. Jornet and I. F. Akyildiz, "Channel modeling and capacity analysis for electromagnetic wireless nanonetworks in the terahertz band," *Wireless Communications, IEEE Transactions on*, vol. 10, no. 10, pp. 3211–3221, 2011.
- [13] I. F. Akyildiz and J. M. Jornet, "Electromagnetic wireless nanosensor networks," *Nano Communication Networks*, vol. 1, no. 1, pp. 3–19, 2010.
- [14] J. M. Jornet, J. C. Pujol, and J. S. Pareta, "Phlame: A physical layer

- aware mac protocol for electromagnetic nanonetworks in the terahertz band,” *Nano Communication Networks*, vol. 3, no. 1, pp. 74–81, 2012.
- [15] K. Yang, A. Pellegrini, M. O. Munoz, A. Brizzi, A. Alomainy, and Y. Hao, “Numerical analysis and characterization of THz propagation channel for body-centric nano-communications,” *IEEE Transactions on Terahertz Science and Technology*, vol. 5, pp. 419–426, May 2015.
  - [16] Y. Feldman, A. Puzenko, P. Ishai, A. Caduff, and A. Agranat, “The electromagnetic response of human skin in the millimetre and submillimetre wave range,” *Phys. Med. Biol.*, vol. 54, pp. 3341–3363, Jun. 2009.
  - [17] K. Yang, Q. Abbasi, N. Chopra, M. Munoz, Y. Hao, and A. Alomainy, “Effects of non-flat interfaces in human skin tissues on the In-Vivo THz communication channel,” *Journal of Nano Communication Network*, Nov., 2015.
  - [18] W. Montagna, *The Structure and Function of Skin 3E*. Elsevier, 2012.
  - [19] I. Hayut, A. Puzenko, P. B. Ishai, A. Polsman, A. J. Agranat, and Y. Feldman, “The helical structure of sweat ducts: Their influence on the electromagnetic reflection spectrum of the skin,” *Terahertz Science and Technology, IEEE Transactions on*, vol. 3, no. 2, pp. 207–215, March 2015.
  - [20] G. Shafirstein and E. G. Moros, “Modelling millimetre wave propagation and absorption in a high resolution skin model: the effect of sweat glands,” *Physics in medicine and biology*, vol. 56, no. 5, p. 1329, 2011.
  - [21] O. Sushko, “Terahertz dielectric study of bio-molecules using time-domain spectrometry and molecular dynamics simulations,” *PhD Thesis, Queen Mary University of London*, 2014.
  - [22] J. R. Birch and E. A. Nicol, “The *fir* optical constants of the polymer *tpx*,” *Infrared Phys.*, vol. 24, pp. 573 – 575, 1984.
  - [23] T. D. Dorney, R. G. Baraniuk, and D. M. Mittleman, “Material parameter estimation with THz time-domain spectroscopy,” *J. Opt. Soc. Am. A*, vol. 18, pp. 1562–1571, 2001.
  - [24] N. Chopra, A. Alomainy, and M. Philpot, “Investigating electromagnetic material properties of collagen at THz for health monitoring applications,” in *MobiHealth 2015*. EAI, 2015.
  - [25] S. Kay, *Fundamentals of statistical signal processing: estimation theory*. Prentice-Hall, 1993.